Radiation Measurements 106 (2017) 3–12

Contents lists available at ScienceDirect

Radiation Measurements

journal homepage: www.elsevier.com/locate/radmeas

An overview of recent developments in luminescence models with a focus on localized transitions

Vasilis Pagonis [a, *], Reuven Chen [b], Christopher Kulp [c], George Kitis [d]

[a] McDaniel College, Physics Department, Westminster, MD 21157, USA
[b] Raymond and Beverly Sackler School of Physics and Astronomy, Tel-Aviv University, Tel-Aviv 69978, Israel
[c] Department of Astronomy and Physics, Lycoming College, Williamsport, PA 17701, USA
[d] Nuclear Physics Laboratory, Aristotle University of Thessaloniki, 54124 Thessaloniki, Greece

HIGHLIGHTS

- Overview of recent developments in localized vs delocalized models.
- New model for luminescence in quartz applicable for from microseconds to seconds.
- Monte Carlo simulations of ground state tunneling in random distribution of defects.

ARTICLE INFO

Article history:
Received 26 September 2016
Received in revised form
19 December 2016
Accepted 9 January 2017
Available online 10 January 2017

Keywords:
Localized luminescence models
Time resolved luminescence
Feldspar models
Quartz models

ABSTRACT

Advances in modeling during the past 20 years have contributed to better understanding of the luminescence properties of dosimetric materials. Three types of models have been used extensively in the literature: delocalized models based on transitions involving the conduction and valence bands, localized models usually involving different energy levels of the same trap, and semilocalized models which are based on a combination of localized and delocalized energy levels. The purpose of this paper is to provide an overview of recent developments in luminescence models, with an emphasis on the importance of delocalized transitions. Two recent theoretical developments are discussed, namely analytical equations based on the Lambert W-function which are applicable for delocalized models, and analytical equations based on tunneling in a random distribution of defects which are applicable for localized models. A new model for luminescence in quartz is proposed, which is applicable for time scales ranging from microseconds to seconds. Recent Monte Carlo simulations of ground state tunneling in a random distribution of traps and centers are discussed, which are based on a modified version of a previously published model. Some of the current challenges associated with luminescence signals measured at elevated temperatures are pointed out, and suggestions are made for future work in this research area.

1. Introduction

Advances in modeling during the past 20 years have contributed to better understanding of the luminescence properties of dosimetric materials. In general terms, luminescence signals from dosimetric materials are characterized by the presence of several components, originating from different traps or centers. These signals vary according to preconditioning of the samples (irradiation dose, prior optical and thermal stimulation, radiation quality). The main goals of modeling studies are: to provide a quantitative description of these dosimetric signals, to develop methods for the accurate evaluation of parameters characterizing traps and centers, to search for general models which explain the behavior of preconditioned samples, and to help researchers understand the underlying luminescence production mechanisms. Three types of models have been used extensively in the literature: delocalized models based on transitions involving the conduction and valence bands, localized models usually involving different energy levels of the traps/centers, and semilocalized models which are based on a combination of localized and delocalized energy levels. For a comprehensive historical summary of these three types of luminescence models, the reader is referred for example to the recent

* Corresponding author.
E-mail address: vpagonis@mcdaniel.edu (V. Pagonis).

http://dx.doi.org/10.1016/j.radmeas.2017.01.001
1350-4487/

review paper by Horowitz et al. (2015) and the book by Chen and Pagonis (2011).

In terms of the time scales involved in luminescence processes, one can distinguish two broad types of experiments. In the first category one studies phenomena like thermoluminescence (TL) or optically stimulated luminescence (OSL) which take place in time scales of seconds. In the second category of time-resolved (TR) experiments, one uses short light pulses to separate the stimulation and emission of luminescence in time. TR experiments usually involve much shorter time scales than TL/OSL, typically of the order of milliseconds or microseconds.

The purpose of this paper is to provide an overview of recent developments in luminescence models, with an emphasis on the importance of delocalized transitions. The paper is organized as follows. Section 2 summarizes two recent theoretical developments, namely analytical equations based on the Lambert W-function which are applicable for delocalized models (Kitis and Vlachos, 2013), and analytical equations based on tunneling in a random distribution of defects, and which are applicable for localized models (Kitis and Pagonis, 2013). Section 3 proposes a new model for luminescence in quartz, which is applicable for time scales ranging from microseconds to seconds. Section 4 is a review of recent research on two different descriptions of ground state tunneling phenomena in a random distribution of defects; a macroscopic differential equations approach, and a microscopic Monte Carlo approach. Finally, section 5 discusses some of the current challenges associated with luminescence signals measured at elevated temperatures, and suggestions are made for future work in this research area.

2. Developments in new analytical equations for localized and delocalized models

In this section we summarize two recent theoretical works on analytical equations which can be used for describing luminescence signals.

2.1. Analytical solutions for the OTOR model using the Lambert function

The OTOR model (one-trap one-recombination center) shown in Fig. 1 is the simplest model describing luminescence and is based on delocalized transitions. The differential equations governing the traffic of electrons between the one trapping level, the recombination center and the conduction band are described in detail in Chen and Pagonis (2011). The OTOR rate equations cannot be solved in closed form. However, by using the simplifying quasi-equilibrium (QE) conditions it is possible to reduce the system of equations in the OTOR model into the following single equation known as the general one trap model (GOT):

$$I(t) = -\frac{dn}{dt} = p(t)\frac{n^2}{(N-n)R+n}, \tag{1}$$

where N (cm^{-3}) is the total concentration of electron traps in the crystal, n_c and n (cm^{-3}) correspondingly are the instantaneous concentrations of electrons in the conduction band and in the filled traps, A_n and A_m ($cm^3 s^{-1}$) are the re-trapping and recombination rates, and $R = A_n/A_m$ is the retrapping ratio. The quantity $p(t)$ (s^{-1}) is the time rate which depends on the stimulation mode used during the experiments. For the case of isothermal excitation and optically stimulated luminescence (OSL), $p(t) = constant$. For the case of thermoluminescence (TL) the quantity $p(t) = sexp(-E/k_BT)$ where E,s are the thermal kinetic parameters characterizing the traps, k_B is the Boltzmann constant and T is the temperature of the sample which is usually increasing linearly with time. The QE conditions used in deriving the GOT model in Equation (1) are $n_c << n$ and $|dn_c/dt| << |dn/dt|$.

Kitis and Vlachos (2013) obtained analytical solutions for equation (1) in terms of the two real branches of the well-known transcendental Lambert function $W(z)$. These two branches of the Lambert function are shown in Fig. 2. These authors found that the two types of solutions depend on the ratio $R = A_n/A_m$ of the re-trapping and recombination rates A_n, A_m. For $R < 1$ the solution of the OTOR model is based on the first real branch of the Lambert function, which is defined in the region $(-1/e) < z < \infty$ and is denoted by W[0,z] in Fig. 2. For $R > 1$ the solution of the OTOR model is based on the second real branch of the Lambert which is defined in the region $(-1/e) < z < 0$ and is denoted by W[-1,z] in Fig. 2. In its most general form the Lambert function is defined as the function satisfying the equation $W(z)e^{W(z)} = z$ for any complex number z. In mathematical form the solution of equation (1) is:

$$I(t) = p(t)\frac{R}{(1-R)^2}\frac{N}{W[k,e^z] + W[k,e^z]^2}, \tag{2}$$

$$z = \frac{NR}{n_o(1-R)}\ln\left(\frac{n_o|1-R|}{NR}\right) + \frac{1}{1-R}\int_{t_o}^{t} p(t)dt \tag{3}$$

where $k = 0$ or $k = -1$ for the two real branches of $W(z)$ correspondingly.

The advantages of using the Lambert function as a deconvolution function for luminescence signals are: (a) Fitting of experimental TL data with the Lambert function produces accurate values of activation energy E (Sadek et al., 2014) (b) $W(z)$ can be used to fit unusual shapes of TL glow curves, where the General Order Kinetics (GOK) and Mixed Order Kinetics (MOK) equations may fail, (c) The Lambert function $W(z)$ is easy to program, since it is already available in many commercial software packages like MATLAB, MINUIT and MATHEMATICA, (d) Analysis of experimental data with $W(z)$ provides a physical interpretation of the luminescence signals based on the retrapping ratio R. By contrast, analysis of data using GOK kinetics is based instead of the empirical kinetic order parameter b which has no direct physical meaning.

This latter case is of major importance, so it will be clarified by an example. A single TL peak is numerically generated using the OTOR model with input parameters $E = 1eV$, $s = 10^{10}\ s^{-1}$, and

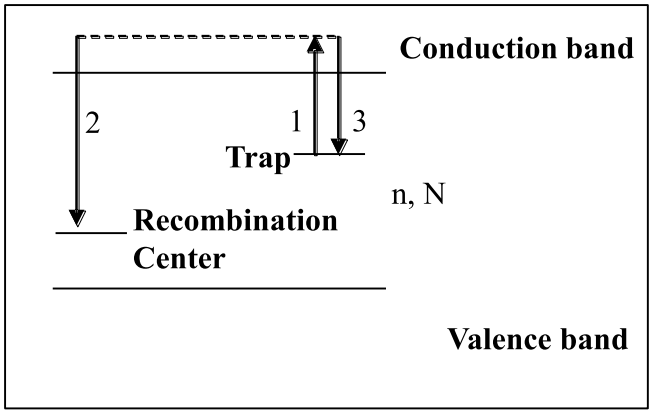

Fig. 1. The delocalized OTOR model containing a single trap and a single recombination center. Transition 1 represents thermal or optical excitation, transition 2 corresponds to the luminescence process from the conduction band into the recombination center, and transition 3 represents the retrapping process.

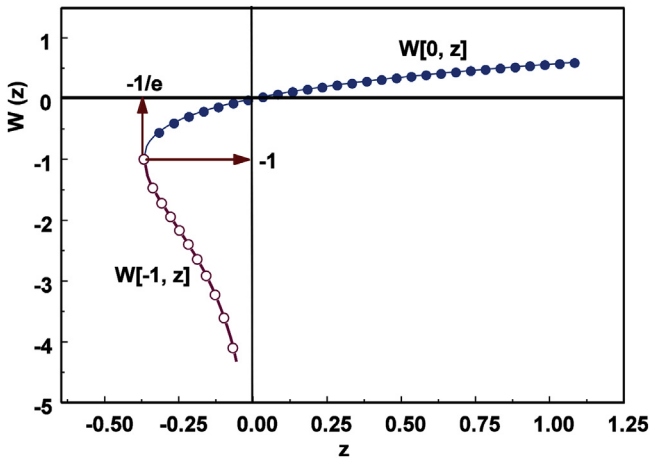

Fig. 2. The two branches of the Lambert W function, showing the different regions of the z parameter for which they are defined.

$n_0 = N = 10^{10} cm^{-3}$, and for two different values of the retrapping ratio $R = 0.25$ and $R = 1000$. Fig. 3 shows that the two calculations produce TL glow curves with very different shapes for the two values of R. These two peaks were fitted using the GOK analytical equations and also using Equation (2) in the form given by Sadek et al., (2015). The TL peak for $R = 0.25$ was fitted using the first branch, and the TL peak for $R = 1000$ using the second branch of the Lambert W function. The open circles represent the simulated peaks and the solid lines the fit by the Lambert equation (2) and by the following well-known GOK equation:

$$I(T) = s'' n_0 \exp\left(-\frac{E}{kT}\right)\left[1 + \frac{s''(b-1)}{\beta}\int_{T_o}^{T} \exp\left(-\frac{E}{kT'}\right)dT'\right]^{-\frac{b}{b-1}} \quad (4)$$

with n_o representing concentration of trapped electrons at time t = 0 (in m^{-3}), b is the general kinetic order parameter, s'' is an empirical parameter acting as an "effective" frequency factor for general order kinetics (in s^{-1}), E is the activation energy (in eV), k = Boltzmann constant (in eV. K^{-1}), t = time (in s), and T is the absolute temperature (in K). A linear heating rate β is used to heat the sample (in $K.s^{-1}$), resulting in the temperature varying as $T = T_o + \beta t$, where T_o is the temperature at time t = 0 (in K).

It is clear that both equations fit both peaks accurately. However, the fitting results shown in the inset table of Fig. 3 indicate that in the case of $R = 0.25$ the Lambert function reproduces exactly the input values of E and R, and gives a FOM value two orders of magnitude better than the GOK method which overestimates the E value by 7%. In the case of $R = 1000$, again both equations give excellent fits. However, the Lambert based fit reproduces the E and R values exactly, whereas the GOK equation gives completely erroneous results of $E = 0.48$ eV instead of the expected value $E = 1$ eV. This example shows that the differences between the GOK equation and the Lambert based analytical equations are of a deeply physical nature, rather than due to mathematical differences between the two fitting models. The correct values of the kinetic parameters are only obtained using the physically meaningful Lambert equation, while the empirical GOK equations fail completely. For further examples of using the Lambert functions, the reader is referred to the recent experiments by Kitis et al. (2016), who used the Lambert W function to fit isothermal luminescence signals in synthetic luminescence materials.

2.2. Localized transitions: the tunneling model of Jain et al. (2012)

A second major recent theoretical development is the model developed by Jain et al. (2012), which has provided a description of tunneling phenomena in a random distribution of electron-hole pairs. The model is shown schematically in Fig. 4a. The main assumptions of the model are the presence of a random distribution of electron-hole pairs, in which the concentration of holes (acceptors) is much larger than the concentration of electrons (donors). Thermal or optical excitation raises the electrons from the ground into the excited state of the system. Tunneling takes place from the

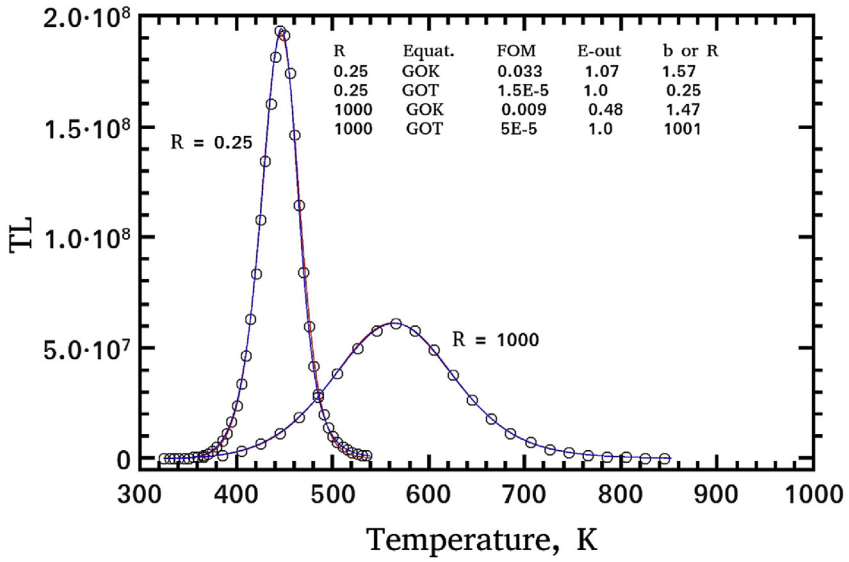

Fig. 3. A single TL peak numerical simulated using the OTOR model for two different values of the retrapping ratio R = 0.25 and 1000, as discussed in the text. The inset table gives the results of fitting the numerically simulated peak using general order kinetics (GOK) and GOT equations. Excellent fits are obtained with both equations, however the GOK model fails to reproduce the correct E values in the model.

excited state of the electron trap into the recombination center, and to the nearest neighbors only. Kitis and Pagonis (2013) quantified the semi-analytical model of Jain et al. (2012) by deriving analytical expressions for different experimental stimulation modes. The analytical equations for excited state tunneling developed by Kitis and Pagonis (2013) are:

$$n(t) = n_o \exp\left[- \rho' F(t)^3 \right] \tag{5}$$

$$F(t) = \ln\left(1 + 1.8 \int_0^t A dt' \right) \tag{6}$$

$$L(t) = -\frac{dn}{dt} = AF(t)^2 \exp[-F(t)] \exp\left[- \rho' [F(t)]^3 \right] \tag{7}$$

where A represents the rate of thermal/optical stimulation, ρ' is the dimensionless charge density, t is the elapsed time since the beginning of experiment, n_o and $n(t)$ are the initial and instantaneous concentration of point defects in the ground state correspondingly. The parameter A has the same physical meaning for different experimental stimulation modes as the parameter $p(t)$ in Equation (1).

The analytical equations (5)–(7) developed by Kitis and Pagonis (2013) were used recently to describe luminescence signals from a variety of feldspars and apatites in a quantitative manner (Polymeris et al., 2014; Sfampa et al., 2014; Pagonis et al., 2014a). Fig. 5a shows a typical example of fitting a continuous wave infrared stimulated luminescence signal (CW-IRSL) from a orthoclase sample with laboratory code VRS3, while Fig. 5b shows an example of a fitted isothermal signal from Durango apatite, measured at 220 °C. For both types of signals Equations (5)–(7) give excellent fits to the experimental data. The experimental setup, sample preparation and experimental conditions for the experiments shown in Fig. 5 were described previously in Polymeris et al. (2014). Luminescence measurements were carried out using a Riso TL/OSL reader (model TL/OSL-DA-15), equipped with a $^{90}Sr/^{90}Y$ beta particle source, delivering a nominal dose rate of 0.075 Gy/s. A 9635QA photomultiplier tube was used with a 7.5 mm Hoya U-340 filter (~340 nm, FWHM ~80 nm), and the IRSL stimulation wavelength is 875 (±40) nm with the maximum power ~135 mW/cm^2. All necessary heating was performed in a nitrogen atmosphere with a low constant heating rate of 2 °C/s, in order to avoid significant temperature lag. For the experiment in Fig. 5a, the irradiated aliquot of sample VRS3 was first preheated to a temperature of 300 °C, followed by measurement of its CW-IRSL signal for 2000 s at 50 °C. For the prompt isothermal measurements reported in Fig. 5b for the Durango apatite, a combination of Pilkington HA-3 heat absorbing and Corning 7–59 (320–440 nm) blue filter were used for light detection. This Durango apatite sample is known to exhibiting strong anomalous fading (Sfampa et al., 2014).

3. Developments in comprehensive empirical models for quartz

This section is organized as follows. Sections 3.1 and 3.2 summarize some of the comprehensive empirical models which have been developed for quartz during the past 10 years. Some of these models are based on *localized* transitions and these have been used to describe time resolved experiments in quartz in the microseconds time scale, while other models are based on *delocalized* transitions and have been used mostly to describe phenomena in the seconds scale. In Section 3.3 we propose a new model for quartz which is based on both localized and delocalized transitions.

3.1. Empirical models for quartz based on localized transitions- time resolved experiments

For a comprehensive review of quartz models based on *localized* transitions the reader is referred to the recent review paper by Chithambo et al. (2016). The main purpose of these types of models is to describe quantitatively time resolved experiments in quartz in the microseconds time scale. Extensive experimental studies of luminescence lifetimes in quartz (see for example Chithambo et al., 2016), have suggested a general energy scheme consisting of three independent radiative luminescence centers denoted by L_H, L_L and L_S, and a non-radiative luminescence center denoted by R. These radiative centers are associated with distinct characteristic lifetimes denoted by τ_H, τ_L and τ_S correspondingly. Time resolved luminescence from sedimentary quartz annealed below 500 °C is dominated by a single component with a luminescence lifetime τ_H ~42 μs, while luminescence in samples annealed above 500 °C is dominated by a characteristic lifetime of τ_L~32 μs. Pagonis et al. (2010) presented a new kinetic model for time resolved experiments which includes thermal quenching in quartz, and which is based on the Mott-Seitz mechanism. In this model all

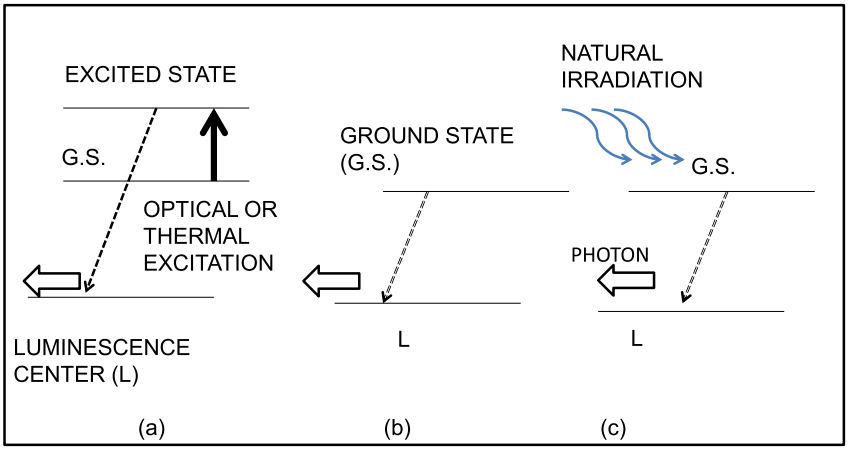

Fig. 4. (a) Tunneling phenomena from the excited state are described by Equation (7) in the text. (b) Tunneling from the ground state are described by Equation (14) in the text. (c) Simultaneous irradiation and tunneling phenomena are described by Equation (15) in the text.

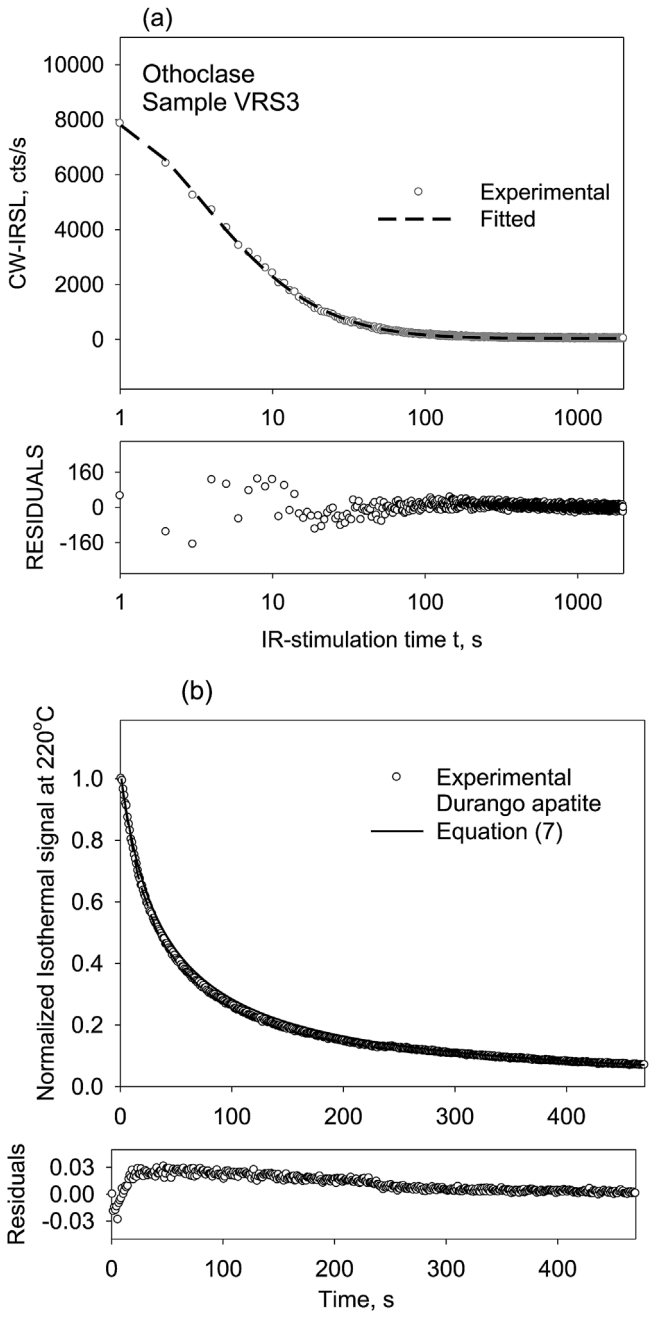

Fig. 5. (a) CW-IRSL experimental data for orthoclase sample VRS3, fitted using Equation (7) in the text. (b) Isothermal experimental data for Durango apatite, fitted using Equation (7) in the text.

recombination transitions are localized *within* the recombination center, in contrast to delocalized models of Section 3.2, in which all charge transitions take place via the conduction and valence bands.

One of the main challenges for these localized transition models is the inclusion of thermal quenching effects, which are well known experimentally in quartz and other dosimetric materials (Nikiforov et al., 2001; Pagonis et al., 2011a, 2014b). In the quartz model of Pagonis et al. (2010), thermal quenching arises from the competition between radiative and non-radiative electronic transitions taking place within the recombination center. Unfortunately, in quartz the nature of both the traps and luminescence centers are still unknown or uncertain, and are the subject of current research.

As the temperature of the sample is increased, electrons are removed from the excited states according to the Boltzmann factors and this leads to both a decrease of the intensity of the luminescence signal and to a simultaneous decrease of the apparent luminescence lifetime τ_L. The model of Pagonis et al. (2010) successfully describes these variations of the luminescence lifetimes and luminescence intensity when optical stimulation takes place in temperatures between 20 and 200 °C (Chithambo et al., 2016).

Pagonis et al. (2010) showed that their model can also describe luminescence processes in quartz from a time scale of microseconds (for TR-OSL experiments), up to a time scale of seconds (for TL and OSL experiments). No modifications are required in the model in order to transition from one time scale to the other. In later work Pagonis et al. (2014b) expanded this model, in an effort to include the experimentally observed lifetimes τ_H and τ_L for annealed sedimentary quartz samples.

While the comprehensive quartz models described in this section successfully combine localized and delocalized transitions over time scales extending several orders of magnitude, the luminescence mechanism in quartz is known to be very complex, and this has led to the parallel development of several empirical comprehensive models which are based on *delocalized* transitions. One of these models is described in the next subsection.

3.2. Empirical models for quartz based on delocalized transitions-TL and OSL experiments

For a recent comparative review of comprehensive quartz models based on delocalized transitions, the reader is referred to the recent comprehensive paper by Friedrich et al. (2016). The first empirical comprehensive quartz model was developed by Bailey (2001), and it contains 5 electron traps and 4 hole centers. Levels 1–4 in the original Bailey model give rise to TL peaks at ~110 °C, 230 °C and two peaks around 330 °C, and levels 3 and 4 also give rise to OSL signals. Level 5 is a thermally disconnected deep electron center, and levels 6–9 are two hole reservoirs, a stable luminescence center and a non-radiative recombination center correspondingly. The model by Bailey (2001) was expanded by Pagonis et al. (2008) to include two additional levels 10 and 11, in order to simulate the experimentally observed thermally transferred OSL (TT-OSL) signals.

In an extensive simulation study, Pagonis et al. (2011b) showed that the model by Pagonis et al. (2008) can simulate a very wide range of experimental results, as well as various experimental protocols used for several TL/OSL dating techniques. This study simulated successfully the following: (a) quantitative description of TL glow curves and their dose response, (b) OSL bleach curves and their dose response (c) the predose technique in quartz, (d) phototransfer phenomena (e) SAR-OSL dating protocol and (f) SAR-TL dating protocols.

The type of delocalized transition model described in this section cannot provide a description of TR-OSL experiments in quartz, which take place in the microseconds time range. Therefore there is a need to *combine* delocalized and localized transitions in a more comprehensive model, which will cover a wider range of time scales. In the next section we propose such a new comprehensive model for quartz, based on *both* localized and delocalized transitions.

3.3. A proposed new comprehensive model for quartz

Fig. 6 shows a proposed new comprehensive model for quartz, which maintains the mathematical and physical characteristics of both the previous delocalized and localized models discussed in sections 3.1 and 3.2. Level 1 in the model represents a shallow

electron trapping level, which gives rise to a TL peak at ~110 °C with a heating rate of 5 K/s. Level 2 represents a generic "230 °C TL" trap, while Levels 3 and 4 are usually termed the fast and medium OSL components and they yield TL peaks at ~330 °C as well as give rise to OSL signals. Level 5 is a deep electron center which is considered thermally disconnected, and levels 6 and 7 are thermally unstable, non-radiative recombination centers ("hole reservoirs"). Level 8 is a thermally stable, radiative recombination center often termed the "luminescence center" (L) and Level 9 is a thermally stable, non-radiative recombination center termed a "killer" center (K). As discussed above, levels 10 and 11 were introduced in order to simulate the experimentally observed thermally transferred OSL (TT-OSL) signals.

The important localized transitions in the model are shown in the middle of Fig. 6, and are denoted by A_R and A_{NR} by following the notation in the localized quartz model of Pagonis et al. (2010). As discussed in section 3.1, thermal quenching arises from the competition between these radiative (A_R) and non-radiative (A_{NR}) electronic transitions taking place within the recombination center. The equations for the traffic of charge carriers in the new proposed model are as follows:

$$\frac{dn_i}{dt} = n_c(N_i - n_i)A_i - n_i P\theta_{oi}\exp\left[-\frac{E_i^{th}}{k_B T}\right] - n_i s_i \exp\left[-\frac{E_i}{k_B T}\right], \quad (8)$$

$$(i = 1,\ldots 5 \quad \text{and} \quad \text{i} = 10, 11)$$

$$\frac{dn_j}{dt} = n_v(N_j - n_j)A_j - n_j s_j e^{\left(-\frac{E_j}{k_B T}\right)} - n_c n_j B_j, \quad (9)$$

$$j = 6, 7, 9$$

$$\frac{dn_L}{dt} = A_{CB}n_c(N_L - n_L) - A_8 n_v n_L - A_R n_L - n_L A_{NR}\exp(-W/k_B T) - n_L s_L \exp[-E_L/kT] \quad (10)$$

$$\frac{dn_c}{dt} = R - A_{CB}n_c(N_L - n_L) - \sum_{i=1}^{5}\left(\frac{dn_i}{dt}\right) - \sum_{i=10}^{11}\left(\frac{dn_i}{dt}\right) - \sum_{j=6,7,9}(n_c n_j B_j) \quad (11)$$

$$\frac{dn_v}{dt} = \frac{dn_c}{dt} + \sum_{i=1}^{5}\left(\frac{dn_i}{dt}\right) + \sum_{i=10}^{11}\left(\frac{dn_i}{dt}\right) - \sum_{j=6,7,9}\left(\frac{dn_j}{dt}\right) \quad (12)$$

The instantaneous luminescence $I(t)$ resulting from the radiative transition shown in the middle of Fig. 6 is defined as:

$$I(t) = A_R n_L \quad (13)$$

In these equations N_i are the total concentrations of electron traps or hole centers (cm^{-3}), n_i are the instantaneous concentrations of trapped electrons or holes (cm^{-3}), s_i are the frequency factors (s^{-1}), E_i are the electron trap depths below the conduction band or hole trap depths above the valence band (eV), A_i (i = 1…5, and i = 10,11) are the conduction band to electron trap transition probability coefficients ($cm^3\ s^{-1}$), A_j (j = 6…9) are the valence band to hole trap transition probability coefficient ($cm^3\ s^{-1}$), valence band to trap transition probability coefficients ($cm^3\ s^{-1}$) and B_j (j = 6…9) are the conduction band to hole center transition probability coefficients ($cm^3\ s^{-1}$). The photo-eviction constant is θ_{0i} (s^{-1}) at T = ∞, the thermal assistance energy E^{th}_i (eV) and P (s^{-1}) is the rate of optical stimulation. A_R and A_{NR} (s^{-1}) are the radiative and non-radiative transition rates necessary to simulate the thermal quenching process, and their numerical values are taken from Pagonis et al. (2010).

It is noted that Equations (8)–(9) describe exclusively delocalized transitions involving the conduction and valence bands, while Equation (10) refers to the luminescence center (level $j = 8$ in the model), which is based on *localized* transitions, and which is the basis of the new proposed model. A new set of parameters are used in the model to describe localized transitions within the luminescence center. This center is described in terms of *electronic states* and *electronic transitions*, by following the mathematical formalism in Pagonis et al. (2010). By following the notation of Pagonis et al. (2010), let us denote by n_L the concentration of *electrons* in the excited state of the luminescence center, and by N_L the corresponding total concentration of these traps in the crystal. The quantities n_L and N_L are then completely analogous to the quantities n_2 and N_2 in the model of Pagonis et al. (2010).

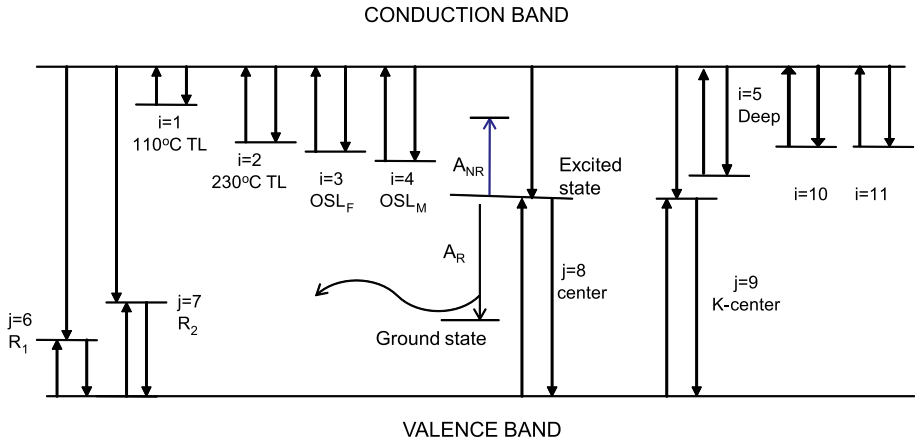

Fig. 6. The new proposed model for quartz, which contains both localized and delocalized transitions. The various transitions and the parameters used in the model are described in the text. This energy scheme describes thermal quenching using the Mott-Seitz mechanism.

It must be emphasized that the key difference between the delocalized model by Pagonis et al. (2008) and the new model is Equation (10), in which the luminescence center is described in terms of *electronic states* and *electronic transitions*, instead of in terms of *holes* and *delocalized transitions*.

Equation (10) describes mathematically five possible transitions involving the electrons in the excited state of the luminescence center, as follows. The first term $A_{CB}n_c(N_L - n_L)$ describes the time rate of electrons being trapped with a rate coefficient A_{CB} from the CB into the excited state n_L. This term is positive, since it leads to an increase of the concentration of electrons n_L in the excited state of the recombination center, by the capturing of electrons from the CB. The second term $-A_8 n_v n_L$ describes holes being trapped with a probability coefficient A_8 from the valence band into the excited electronic state. This term is negative, since it leads to a decrease of the concentration of electrons n_L by the capturing of holes from the VB. The third term $A_R n_L$ describes electrons undergoing the radiative transition from the excited into the ground state of the center, and the fourth term $n_L A_{NR} \exp(-W/k_B T)$ describes the non-radiative localized transition which competes for electrons from the excited state. The last term $n_L s_L e^{-E_L/kT}$ describes the thermal properties of the electrons in the excited state, using the frequency coefficient s_L and thermal activation energy E_L. It is noted that the above equation (10) for dn_L/dt contains both localized and delocalized transitions.

When using the model in Fig. 6 with the original values of the parameters in Pagonis et al. (2008), it was found that the conduction band empties very slowly, on a time scale of ~0.1 s. This value is in contradiction to several experimental and simulation studies, which show that the CB probably empties much faster, perhaps within a few microseconds (Chithambo et al., 2016). This deficiency of this type of model was discussed in Pagonis et al. (2010, page 909), and is due to the very low values of total concentrations of electrons used in the empirical quartz models. In order to achieve a free carrier lifetime of $\tau \sim 1$ μs, it was found necessary to increase the values of *all electron and hole concentrations* in the model by a factor of $5x10^4$, while leaving all other parameters in the model unchanged. From a physical point of view, when using higher values of the total concentrations of carriers in the model, all processes in the system will take place much faster, but the relative distribution of electrons and holes in the various traps and centers remains the same. The final values of all parameters used in the new comprehensive model of Fig. 6 are shown in Table 1.

The new model shown in Fig. 6 was tested extensively, and it provides a quantitative description of luminescence phenomena in quartz from microseconds up to seconds. Specifically, the new model can describe (a) TR-OSL experiments (in the microseconds time range) as shown in Fig. 7, (b) TL experiments in the seconds time range including thermal quenching, as shown in Fig. 8, and (c) the complex TT-OSL quartz dating protocol discussed in Pagonis et al. (2011b) is shown in Fig. 9. In summary, the new model maintains the physical and mathematical properties of the earlier models, by using both their localized and delocalized characteristics. Further testing of the model and comparison with experimental data is in progress and will be presented elsewhere.

Table 1
Kinetic parameters for the new proposed model shown in Fig. 4. The various parameters are discussed in the text.

	N_i cm^{-3}	E_i eV	s_i s^{-1}	A_i $cm^3 s^{-1}$	B_i	θ_{0i} s^{-1}	E_i^{th} eV
1	7.5e11	0.97	5e12	1e-8		0.75	1
2	5e11	1.55	5e14	1e-8		0	0
3	2e12	1.73	6.5e13	5e-9		6	0.1
4	1.2e13	1.8	1.5e13	5e-10		4.5	0.13
5	2.5e15	2	1e10	1e-10		0	0
6	1.5e13	1.43	5e13	5e-7	5e-9	0	0
7	5e14	1.75	5e14	1e-9	5e-10	0	0
8	1.5e15	5	1e13	1e-10	1e-10	0	0
9	6 e16	5	1e13	1e-14	3e-10	0	0
10	2.5e14	1.65	3.9e13	1e-11		0.01	0.2
11	2e14	1.6	5e12	6e-12		0	0

4. Models of ground state tunneling in random distributions of defects

This section presents a general overview of ground state tunneling phenomena in systems of random defects. Quantum mechanical tunneling and the associated phenomenon of "anomalous fading" of luminescence signals are now well established as dominant mechanisms in feldspars and apatites (Pagonis and Kitis, 2015). Two types of tunneling processes have been investigated experimentally and by the development of appropriate models. The first type of quantum mechanical tunneling is considered to take place directly from the ground state of the trap, as shown in Fig. 4b. The second type of quantum mechanical tunneling is considered to take place via the excited state of the system of electron-hole pairs, and was discussed briefly in Section 2.2 of this paper and shown in Fig. 4a. Two possible complementary modeling approaches have been used in the literature to simulate ground state tunneling in random distribution of defects: a *macroscopic* description using

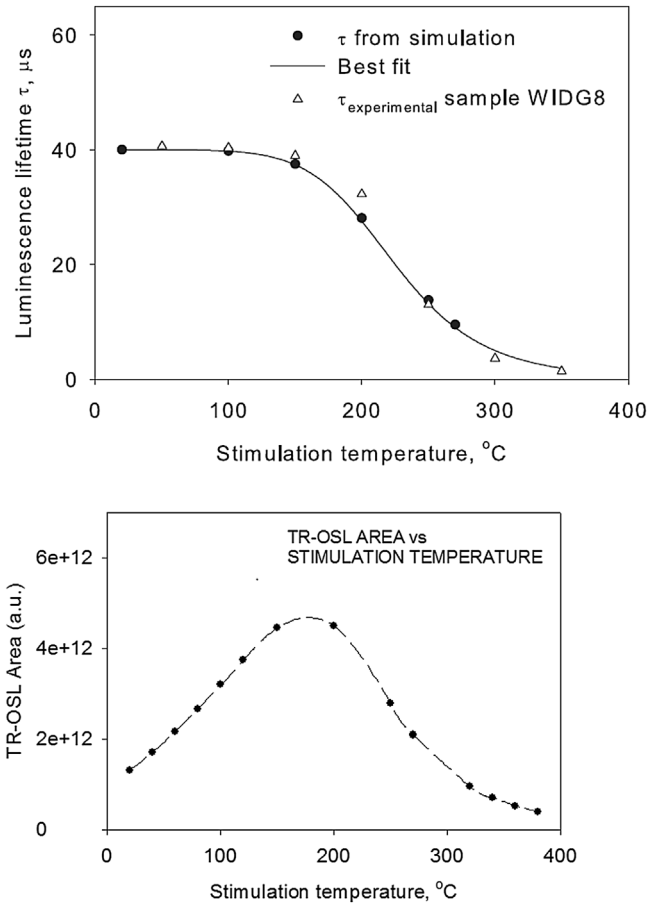

Fig. 7. Time resolved (TR) experimental data for quartz, in the microseconds scale. (a) Luminescence lifetime as a function of the stimulation temperature and (b) Total TR-OSL area as a function of stimulation temperature. The solid lines represent the best fits obtained from the new proposed model in Fig. 6.

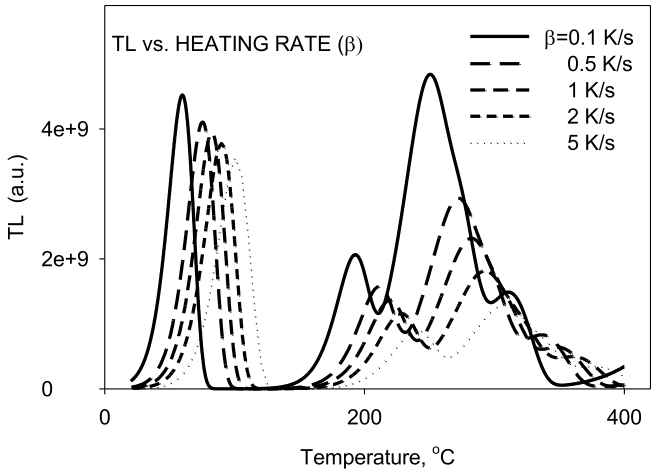

Fig. 8. Simulated TL quartz data in the seconds scale for different heating rates β, demonstrating the effect of thermal quenching. These simulated data were also obtained from the new proposed model in Fig. 6.

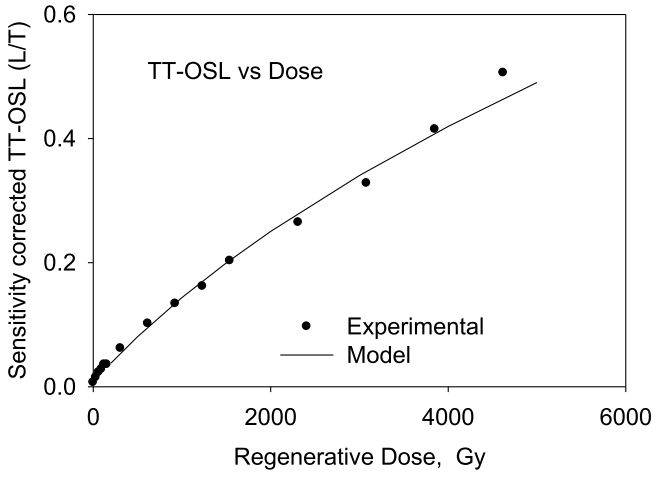

Fig. 9. Simulated TT-OSL protocol dose response, obtained with the model shown in Fig. 6.

differential equations, and a *microscopic* descriptions based on Monte Carlo simulations. These two approaches are discussed in the next two subsections.

4.1. Ground state tunneling in random defects: the differential equation approach

The differential equation description of ground state tunneling is now well established and provides a macroscopic description of the system. Recently Pagonis and Kitis (2015) considered mathematical aspects of the two ground state tunneling models by Huntley (2006) and by Li and Li (2008), shown in Fig. 4b and c correspondingly. The loss of charge in a distribution of random defects is described by the following well-known analytical equation (Tachiya and Mozumder, 1974; Huntley, 2006):

$$n(t) = n_o \exp\left[- \rho' \ln(1.8st)^3 \right], \tag{14}$$

where ρ' is the dimensionless charge density describing the system and s is the tunneling frequency. Pagonis and Kitis (2015) developed the following new analytical equation describing the effect of anomalous fading on the dose response curves (DRCs) of naturally irradiated samples, based on the model by Li and Li (2008) shown in Fig. 4c:

$$L_n(D_n) = \left[1 - \exp\left[- \frac{D_n}{D_0} \right]\right] M \exp\left[- \rho' \ln\left[\frac{D_o s}{D_R}\right]^3 \right] \tag{15}$$

where L_n is the luminescence signal, D_n is the natural irradiation dose (Gy), D_o is the characteristic dose (Gy), M is the total number of traps, D_R is the natural irradiation rate (Gy/ka) and s (s^{-1}) is the tunneling frequency.

4.2. Ground state tunneling in random defects: the Monte Carlo approach

In this subsection we describe a different modeling approach based on Monte Carlo techniques. There have been several efforts to develop models for luminescence signals in feldspars, based on a random distribution of donor-acceptor pairs. One of the basic assumptions of these models is that whenever an electron trap is occupied, the electron will always have the same nearest hole with which to recombine, i.e. the number density of trapped holes in the phosphor is assumed to be much larger than the concentration of trapped electrons. Larsen et al. (2009) presented a numerical Monte Carlo model that simulated the processes of charge loss, charge creation and charge recombination in feldspar. In contrast to the assumptions made by previous analytical models, they assumed that the number density of electrons and holes are equal at all times. The focus of their study was to reproduce the experimentally observed values of the well-known g-factor describing anomalous fading effects. These authors were not able to get reliable results for bulk crystals, and obtained good agreement with experiment only when they assumed that the material consisted of small nanocrystals, and that charge carriers were allowed to recombine only within these smaller volumes.

Pagonis and Kulp (2017) presented a different version of the model by Larsen et al. (2009), in which the number density of acceptors far exceeds that of donors. The new version of the model was used to simulate the loss of charge due to ground state tunneling, as well as the charge creation by natural irradiation of the samples. The results from the model compared well with the analytical equations (14) and (15) presented in the previous subsection. The simulations can describe the loss of charge on a wide variety of time scales, from microseconds to thousands of years. The effect of crystal size, charge carrier density, natural irradiation dose rate and total number of charge carriers were studied in a quantitative manner. Finally, Pagonis and Kulp (2017) examined the possibility of extending the version of the model to describe luminescence signals originating in the nearest neighbor hopping mechanism in feldspars. The results from the model were compared with experimental data from time-resolved infrared stimulated luminescence (TR-IRSL) in these materials.

The Monte Carlo simulations can provide valuable insight into the various factors which affect the luminescence mechanism in these materials. Fig. 10 shows an interactive simulation of the effect of various parameters on the loss of charge in feldspars (Kulp and Pagonis, 2016). The simulation consists of several “buttons” which can be activated in any sequence by the user, to investigate the changes taking place in the curve *n(t)* describing the loss of charge due to ground state tunneling. In Fig. 10 these buttons vary the tunneling frequency *s*, the potential barrier penetration constant α, the dimensions of the cube and the number of Monte Carlo runs (number of solids). The solid line in Fig. 10 represents the analytical

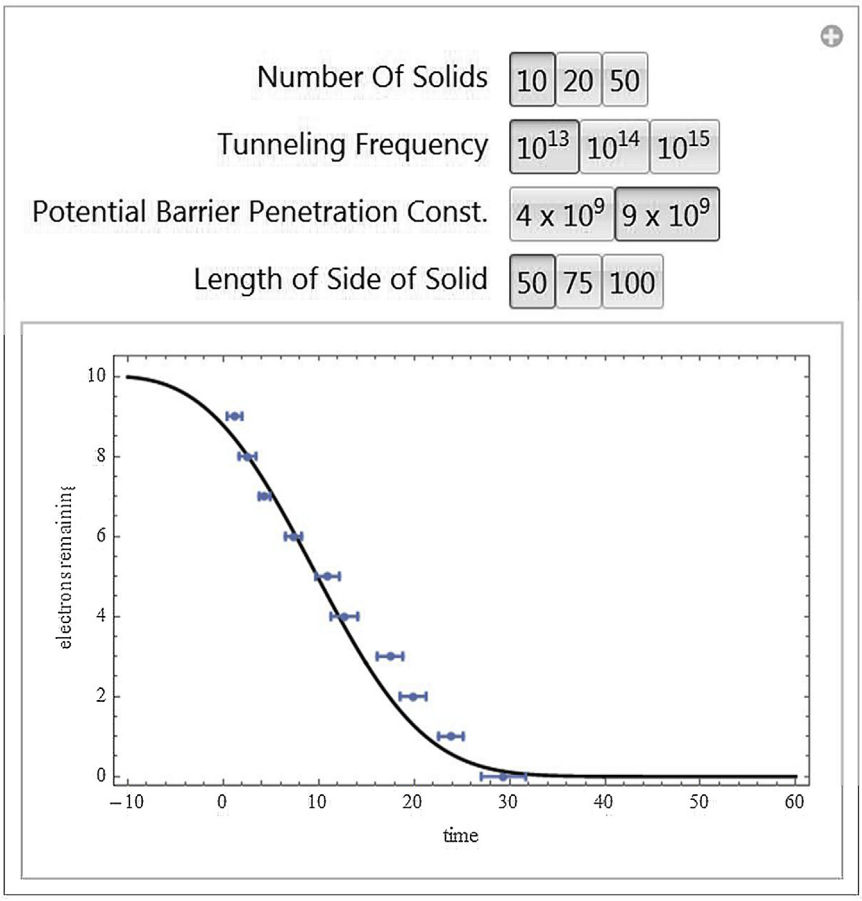

Fig. 10. Interactive demonstrations of ground state tunneling. The user can vary the various parameters in the model and immediately see the effect of each parameter in the loss of charge over time. Variation of the parameters is achieved by activating the various "buttons" shown here. The solid line represents the analytical equation (14).

equations described by the analytical equation (14). The simulations were developed by using the command *Manipulate* in *Mathematica*. The computer code for the interactive demonstrations in Fig. 10 are available to all users via the *Wolfram Demonstration Project*, a web-based open-access collection of interactive scientific animations (Kulp and Pagonis, 2016).

The advantages of using a Monte Carlo method, as opposed to the differential approach, are (Pagonis and Kulp, 2017):

(a) the method is fast, efficient and avoids numerical integrations required in the differential equation approach.
(b) it can be used to produce accurate results in cases of low stimulation probability, in which it is known that the analytical equations of Kitis and Pagonis (2013) fail.
(c) it can be used for both freshly irradiated samples and for irradiated samples which underwent thermal or optical pretreatments.
(d) it can also be used to describe time-resolved experiments based on Mott hopping processes (Mott and Davis, 1979).

5. Conclusions and future challenges in luminescence modeling

This paper has presented an overview of recent developments in luminescence modeling. Section 2 summarized presented recent theoretical developments based on the Lambert W-function, and how this mathematical function can be used to fit experimental TL, OSL and LM-OSL data based on delocalized transitions within the GOT model. The availability of the analytical Lambert solutions for the GOT model presents a significant mathematical step in the development and understanding of basic processes based on delocalized transitions, and how they may be distinguished experimentally from localized transitions. For example, recent work has shown that it may be possible for experiments to distinguish between localized and delocalized processes in a material, by analyzing isothermal TL signals assuming different models (Kitis et al., 2016).

Similarly, in the case of localized tunneling transitions for random distributions of defects, the analytical equations developed by Kitis and Pagonis (2013) based on the model by Jain et al. (2012), represent a new rich area of research which is still being explored both experimentally and with modeling work. This work has led to a better understanding of *ground state* tunneling phenomena in feldspars, apatites and similar natural and synthetic luminescence materials. However, there is much work to be done in order to understand the associated phenomena of tunneling from the *excited state* of the electron-hole pair in a luminescence material.

Closely associated with tunneling from the excited state of the electron-hole pair are two fundamental areas of research which are of importance for both luminescence dating and luminescence dosimetry. These are the temperature dependence of the luminescence signal in feldspars and apatites, and the exact nature of

the various luminescence pathways including the band tail states in these materials. Understanding these various pathways is a key part of improving the various proposed experimental protocols for dating these materials (postIR-IR protocols, MET-IR protocols etc).

Section 3 presented a new model for luminescence in quartz, which is applicable for time scales ranging from microseconds to seconds. This type of model which combines localized and delocalized transitions could also be applicable to the study of luminescence signals from materials like YPO_4 double doped with lanthanides. These materials exhibit temperature dependent tunneling phenomena and apparently can be described by a combination of localized and delocalized transitions. Often such materials also demonstrate the anomalous heating rate effect, in which the area under a TL glow curve increases with heating rate, instead of the opposite behavior that one sees in materials with thermal quenching (Mandowski and Bos, 2011).

Section 4 in this paper presented two different descriptions of *ground* state tunneling phenomena in a random distribution of defects; a macroscopic differential equations approach, and a microscopic Monte Carlo approach. Both of these approaches can easily be extended for the case of excited state tunneling. While the differential equation approach has been well studied, little work has been done on the relevant Monte Carlo research for tunneling materials. This is an area where future research can yield new results, of importance to both fundamental understanding of tunneling luminescence and for practical dosimetry applications.

References

Bailey, R., 2001. Towards a general kinetic model for optically and thermally stimulated luminescence of quartz. Radiat. Meas. 33, 17–45.

Chen, R., Pagonis, V., 2011. Thermally and Optically Stimulated Luminescence: a Simulation Approach. Chichester: Wiley and Sons.

Chithambo, M., Ankjærgaard, C., Pagonis, V., 2016. Time-resolved luminescence from quartz: an overview of contemporary developments and applications. Phys. B 481, 8–18.

Friedrich, J., Kreutzer, S., Schmidt, C., 2016. Solving ordinary differential equations to understand luminescence: 'RLumModel', an advanced research tool for simulating luminescence in quartz using R. Quat. Geochronol. 35, 88–100.

Horowitz, Y.S., Eliyahu, I., Oster, L., 2015. Kinetic simulations of thermoluminescence dose response: long overdue confrontation with the effects of ionization density. Rad. Prot. Dosim. 1–17. http://dx.doi.org/10.1093/rpd/ncv495.

Huntley, D.J., 2006. An explanation of the power-law decay of luminescence. J. Phys. Condens. Matter 18, 1359.

Jain, M., Guralnik, B., Andersen, M.T., 2012. Stimulated luminescence emission from localized recombination in randomly distributed defects. J. Phys. Condens. Matter 24, 385402 (12pp).

Kitis, G., Pagonis, V., 2013. Analytical solutions for stimulated luminescence emission from tunneling recombination in random distributions of defects. J. Lum. 137, 109–115.

Kitis, G., Vlachos, N.D., 2013. General semi-analytical expressions for TL, OSL and other luminescence stimulation modes derived from the OTOR model using the Lambert W-function. Radiat. Meas. 48, 47–54.

Kitis, G., Polymeris, G.S., Sfampa, I.K., Prokic, M., Meriç, N., Pagonis, V., 2016. Prompt isothermal decay of thermoluminescence in MgB_4O_7:Dy,Na (MBO) and LiB_4O_7:Cu, in (LBO). Radiat. Meas. 84, 15–25.

Kulp, C., Pagonis, V., 2016. Interactive Monte Carlo Demonstrations of Ground State Tunneling Phenomena in Solids. Published in the Wolfram Demonstration Project. http://demonstrations.wolfram.com/MonteCarloModelOfChargeRecombinationInFeldspars/.

Larsen, A., Greilich, S., Jain, M., Murray, A.S., 2009. Developing a numerical simulation for fading in feldspar. Radiat. Meas. 44, 467.

Li, B., Li, S.H., 2008. Investigations of the dose-dependent anomalous fading rate of feldspar from sediments. J. Phys. D. Appl. Phys. 41, 225502.

Mandowski, A., Bos, A.J.J., 2011. Explanation of anomalous heating rate dependence of thermoluminescence in YPO_4:Ce^{3+}, Sm^{3+} based on the semi-localized transition (SLT) model. Radiat. Meas. 46, 1376–1379.

Mott, N.F., Davis, E.A., 1979. Electronic Processes in Non-crystalline Materials, second ed. Clarendon Press, Oxford, pp. 216–218.

Nikiforov, S.V., Milman, I.I., Kortov, V.S., 2001. Thermal and optical ionization of F-centers in the luminescence mechanism of anion-defective corundum crystals. Radiat. Meas. 33, 547.

Pagonis, V., Kitis, G., 2015. Mathematical aspects of ground state tunneling models in luminescence materials. J. Luminescence 168, 137–144.

Pagonis, V., Kulp, C., 2017. Monte Carlo simulations of tunneling phenomena and nearest neighbor hopping mechanism in feldspars. J. Lumin. 81, 114–120.

Pagonis, V., Wintle, A.G., Chen, R., Wang, X., 2008. A theoretical model for a new dating protocol for quartz based on thermally transferred OSL (TT-OSL). Radiat. Meas. 43, 704–708.

Pagonis, V., Ankjærgaard, C., Murray, A.S., Jain, M., Chen, R., Lawless, J., Greilich, S., 2010. Modelling the thermal quenching mechanism in quartz based on time-resolved optically stimulated luminescence. J. Lumin 130, 902–909.

Pagonis, V., Chen, R., Maddrey, J.W., Sapp, B., 2011a. Simulations of time-resolved photoluminescence experiments in a-Al2O3:C. J. Lumin 131, 1086–1094.

Pagonis, V., Chen, R., Kitis, G., 2011b. On the intrinsic accuracy and precision of luminescence dating techniques for fired ceramics. J. Archaeol. Sci. 38, 1591–1602.

Pagonis, V., Jain, M., Thomsen, K.J., Murray, A.S., 2014a. On the shape of continuous wave infrared stimulated luminescence signals from feldspars: a case study. J. Lum 153, 96–103.

Pagonis, V., Chithambo, M.L., Chen, R., Chruścińska, A., Fasoli, M., Li, S.H., Martini, M., Ramseyer, K., 2014b. Thermal dependence of luminescence lifetimes and radioluminescence in quartz. J. Lumin 145, 38–48.

Polymeris, G.S., Giannoulatou, V., Sfampa, I.K., Tsirliganis, N.C., Kitis, G., 2014. Search for stable energy levels in materials exhibiting strong anomalous fading: the case of apatites, 2014. J. Lumin. 153, 245–251.

Sadek, A.M., Eissa, H.M., Basha, A.M., Kitis, G., 2014. Resolving the limitation of the peak fitting and peak shape methods in the determination of the activation energy of thermoluminescence glow peaks. J. Lumin 146, 418–423.

Sadek, A.M., Eissa, H.M., Basha, A.M., Carinou, E., Askounis, P., Kitis, G., 2015. The deconvolution of thermoluminescence glow curves using general expressions derived from one trap-one recombination (OTOR) level model. Appl. Radiat. Isot. 95, 214–221.

Sfampa, I.K., Polymeris, G.S., Tsirliganis, N.C., Pagonis, V., Kitis, G., 2014. Prompt isothermal decay of thermoluminescence in an apatite exhibiting strong anomalous fading, 2014. Nucl. Meth. Instr. B 320, 57–63.

Tachiya, M., Mozumder, A., 1974. Decay of trapped electrons by tunnelling to scavenger molecules in low temperature glasses. Chem. Phys. Lett. 28, 87–89.